



# Rapid radiative clearing of protoplanetary discs

Thomas J. Haworth,<sup>1</sup><sup>★</sup> Cathie J. Clarke<sup>1</sup> and James E. Owen<sup>2</sup><sup>†</sup>

<sup>1</sup>*Institute of Astronomy, Madingley Rd, Cambridge CB3 0HA, UK*

<sup>2</sup>*Institute for Advanced Study, Einstein Drive, Princeton NJ 08540, USA*

Accepted 2015 December 29. Received 2015 December 23; in original form 2015 December 7

## ABSTRACT

The lack of observed transition discs with inner gas holes of radii greater than  $\sim 50$  au implies that protoplanetary discs dispersed from the inside out must remove gas from the outer regions rapidly. We investigate the role of photoevaporation in the final clearing of gas from low mass discs with inner holes. In particular, we study the so-called ‘thermal sweeping’ mechanism which results in rapid clearing of the disc. Thermal sweeping was originally thought to arise when the radial and vertical pressure scalelengths at the X-ray heated inner edge of the disc match. We demonstrate that this criterion is not fundamental. Rather, thermal sweeping occurs when the pressure maximum at the inner edge of the dust heated disc falls below the maximum possible pressure of X-ray heated gas (which depends on the local X-ray flux). We derive new critical peak volume and surface density estimates for rapid radiative clearing which, in general, result in rapid dispersal happening less readily than in previous estimates. This less efficient clearing of discs by X-ray driven thermal sweeping leaves open the issue of what mechanism (e.g. far-ultraviolet heating) can clear gas from the outer disc sufficiently quickly to explain the non-detection of cold gas around weak line T Tauri stars.

**Key words:** instabilities – protoplanetary discs – circumstellar matter – stars: pre-main-sequence – X-rays: stars.

## 1 INTRODUCTION

Understanding the mechanism by which protoplanetary discs are dispersed is important, in particular, because it constrains the time-scale within which planets can form (Haisch, Lada & Lada 2001; Rice & Armitage 2003). Based on the discovery of discs with inner holes (Dullemond, Dominik & Natta 2001; Calvet et al. 2002), it is now generally thought that disc dispersal happens from the inside out (e.g. Koepferl et al. 2013). Such discs with inner holes have thus been labelled ‘transition discs’. Originally observed as a deficiency in the near-infrared component of the disc spectral energy distribution (which can be explained by a dustless inner hole, still populated by gas) inner holes in the dust have subsequently been directly imaged, verifying their existence (e.g. Andrews et al. 2011). Inner holes in gas have also been observed for some transition discs (e.g. Bruderer et al. 2014; van der Marel et al. 2015). Multiple explanations for the appearance of inner holes have been proposed; however, the most promising are either clearing by a planet (or planets) or photoevaporation (Williams & Cieza 2011).

An enduring puzzle for understanding the clearing of protoplanetary discs is the absence of a significant population of older T Tauri stars which have ceased accreting, lack signatures of an inner

disc but retain residual gas and dust at radii beyond 10 au (Owen & Clarke 2012). Secular disc evolution models that include both accretion on to the star and photoevaporation tend to predict that, once photoevaporation halts the accretion on to the star, a few Jupiter masses of gas should be left at radii beyond 10 au and that this should survive for of order half a Myr thereafter before ultimate photoevaporation (Owen et al. 2010; Owen, Ercolano & Clarke 2011; Owen, Clarke & Ercolano 2012). This prediction runs counter both to the aforementioned lack of non-accreting systems with large holes in the *dust* and also to the low upper limits on *gas* mass ( $\sim 0.1$  Jupiter masses) detected in non-accreting (Weak Line) T Tauri stars (Cieza et al. 2013; Hardy et al. 2015). Apparently then, once accretion ceases, the reservoir of gas at large radii must either be small or else then rapidly cleared by an unidentified mechanism. Throughout this paper, we will refer to the statistics of non-accreting transition discs as providing an observational benchmark for testing models of disc clearing.

Predictions for the sequence of outer disc clearing by photoevaporation have been developed by more than a decade of radiation hydrodynamical modelling involving a range of high energy radiation sources from the central star, though full radiation hydrodynamical modelling is still not available in the case of the FUV (far-ultraviolet, i.e. non-ionizing ultraviolet continuum) owing to the complexity of combining this with the complex thermochemical models in this regime (Gorti & Hollenbach 2009; Gorti, Hollenbach & Dullemond 2015). A number of authors (Hollenbach et al. 1994;

<sup>★</sup> E-mail: [thaworth@ast.cam.ac.uk](mailto:thaworth@ast.cam.ac.uk)

<sup>†</sup> Hubble Fellow.

Clarke, Gendrin & Sotomayor 2001; Alexander, Clarke & Pringle 2006a,b) have studied the effect of photoevaporation by Lyman continuum photons on discs, calculating mass-loss profiles and integrated mass-loss rates. In such models, the properties of the mass flow at the base of the wind are set by imposing ionization equilibrium, taking into account the role of the diffuse field of recombination photons, emitted from the static atmosphere of the inner disc, in irradiating the disc at larger radius. In polychromatic Monte Carlo radiative transfer models using the MOCASSIN code, Ercolano, Clarke & Drake (2009) found that X-rays ( $100 \text{ eV} < h\nu < 1 \text{ keV}$ ) are much more effective at penetrating large columns into the disc than the extreme ultraviolet (EUV,  $10 < h\nu < 100 \text{ eV}$ ) and hence will govern the mass-loss properties of discs unless there are geometrical effects which preferentially obscure the X-ray emission. Owen et al. (2010, 2011, 2012) used MOCASSIN to develop a temperature prescription as a function of the ionization parameter for all gas optically thin to the soft ( $< 1 \text{ keV}$ ) X-rays (defined as that within the column of  $10^{22} \text{ particles cm}^{-2}$  from the star). They applied this prescription to new models of disc photoevaporation for different star and disc masses.

Owen et al. (2012) also unexpectedly found that for a particularly low-mass disc, dispersal was very rapid (on time-scales of order hundreds of years) by a mechanism that they termed ‘thermal sweeping’. The key point here is that very rapid dispersal of gas in the outer disc, once the surface density has fallen below a given threshold, offers the prospect of being able to explain the lack of significant gas reservoirs around non-accreting stars. Owen et al. (2012, 2013) proposed analytic expressions for the threshold for thermal sweeping which involved equating the radial scalelength of X-ray heated gas ( $\Delta$ ) with the vertical scaleheight ( $H$ ). The resulting surface density thresholds were used both in these papers and by Rosotti, Ercolano & Owen (2015) in order to explore how such sweeping affects the statistics of gas/dust detection around non-accreting T Tauri stars. Nevertheless, it needs to be stressed that these analytic expressions were based on a simple criterion for thermal sweeping ( $\Delta/H = 1$ ) that was inferred from only two, two-dimensional, radiation hydrodynamical simulations (in the limit of low stellar mass and high X-ray luminosity) and therefore one should be cautious about extrapolating these conditions to different physical regimes.

Accordingly, in this paper, we perform a suite of radiation hydrodynamical simulations which explore the conditions required for rapid radiative disc dispersal, in particular testing the suggestion of Owen et al. (2012) that rapid clearing is triggered once  $\Delta/H$  rises to a value of around unity. We find that although rapid clearing is indeed associated with large  $\Delta/H$  values, stable mass-loss can still ensue when  $\Delta/H$  is greater than unity. Furthermore, we find that  $\Delta/H$  is not always sensitive to the disc surface density. We explore the reason for this difference compared to the work by Owen et al. (2013), develop a new criterion for rapid disc dispersal and discuss the consequences of the new criterion.

The structure of the paper is as follows. In Section 2, we review the rationale behind the surface density criteria previously proposed by Owen et al (2012, 2013). Sections 3 and 4 contain the details and testing of our numerical implementation. In section 5, we present our main simulation results, show that the previous thermal sweeping theories are inadequate and introduce and test a new criterion for rapid disc clearing. In section 6, we discuss the consequences of our new thermal sweeping criterion on populations of viscous discs undergoing internal photoevaporation. Our summary and main conclusions are presented in section 7.

## 2 THE PRIOR THEORY OF THERMAL SWEEPING

Owen et al. (2012) proposed a criterion for thermal sweeping involving equality between the radial pressure scalelength in the X-ray heated gas ( $\Delta = 1/\frac{d \log P}{dR}$ ) and the local vertical pressure scalelength ( $H = 1/\frac{d \log P}{dz} \sim c_s/\Omega$ ). Assuming that X-rays penetrate through to the surface density peak close to the disc inner edge  $\Sigma_{\text{max}}$  and that the X-ray heated column at the disc inner edge is  $10^{22} \text{ cm}^{-2}$ , imposing pressure balance at the X-ray heated interface gives a critical surface density for thermal sweeping of

$$\Sigma_{\text{TS}} = 0.43 \text{ g cm}^{-2} \left( \frac{\mu}{2.35} \right) \left( \frac{T_X}{400 \text{ K}} \right)^{1/2} \left( \frac{T_D}{20 \text{ K}} \right)^{-1/2}, \quad (1)$$

where  $\mu$ ,  $T_X$  and  $T_D$  are the mean molecular weight and X-ray heated and dust temperatures respectively.

Owen et al. (2013) attempted a more rigorous analysis of the criterion for the onset of thermal sweeping, specifically addressing two assumptions used in their original approach.

(i) Relaxing the assumption that the column of X-ray heated gas to the star is always  $10^{22} \text{ cm}^{-2}$  (we refer to this as being ‘column limited’) and allowing instead for the possibility that the density is sufficiently high that the X-rays cannot heat the gas above the dust temperature. We refer to this latter scenario as being ‘density limited’.

(ii) Relaxing the assumption that the dust to X-ray heated transition occurs at the peak surface density of the disc. Instead the transition from X-ray heated to dust heated gas is located self-consistently at some radius interior to that of peak surface density.

In recognition of the fact that the flow near the disc rim is nearly radial, Owen et al. (2013) solved for 1D steady state flows with mass-loss rates set by conditions at the X-ray sonic surface. Such flows are highly subsonic in the vicinity of the disc rim and thus the structure in this region (which is important for assessing the onset of thermal sweeping in 2D) is close to one of hydrostatic equilibrium. This allowed Owen et al. (2013) to propose analytic criteria for the onset of thermal sweeping (i.e. assuming that this occurs when  $\Delta = H$ ) in both the density limited and column limited regimes. They found that (in contrast to the hypothesis in Owen et al. 2012) the X-ray heated interface is generally set by the density limited criterion and that in this case the critical peak surface density *increases* with inner hole radius and X-ray luminosity. Motivated by these findings they developed an ‘improved’ criterion for thermal sweeping which we give below (correcting typos in Owen et al 2013):

$$\begin{aligned} \Sigma_{\text{TS}} = & 0.033 \text{ g cm}^{-2} \left( \frac{L_X}{10^{30} \text{ ergs}^{-1}} \right) \left( \frac{T_{1\text{au}}}{100 \text{ K}} \right)^{-1/2} \\ & \times \left( \frac{M_*}{M_\odot} \right)^{-1/2} \left( \frac{R_{\text{max}}}{\text{au}} \right)^{-1/4} \\ & \times \exp \left[ \frac{1}{2} \left( \frac{R_{\text{max}}}{\text{au}} \right)^{1/2} \left( \frac{T_{1\text{au}}}{100 \text{ K}} \right)^{-1} \right], \end{aligned} \quad (2)$$

where  $L_X$ ,  $T_{1\text{au}}$ ,  $R_{\text{max}}$  are the X-ray luminosity of the star, the dust temperature at 1 au and the radius of maximum surface density (which is assumed to be coincident with the inner hole radius).

The exponential term in the above expression causes the critical surface density to increase with radius (see the blue line in Fig. 8 of this paper); this would imply an important role for thermal sweeping at large radius even for models with relatively high

surface density normalization. When this criterion was combined with plausible models for disc secular evolution it was predicted that thermal sweeping should limit maximum hole sizes in X-ray luminous sources to around 25–40 au.

### 3 NUMERICAL METHOD

We perform radiation hydrodynamic (RHD) simulations in this paper using a modified version of the RHD code *TORUS* (Harries 2000; Haworth & Harries 2012; Harries 2015; Haworth et al. 2015). *TORUS* is primarily a Monte Carlo radiation transport code, though no Monte Carlo radiative transfer is used in this paper. Rather we use the same simplified EUV/X-ray heating prescription (based on the ionization parameter in optically thin regions: see 2.2 below) as in Owen et al. (2012), in part to remain consistent with their work but also to reduce the computational expense.

#### 3.1 Hydrodynamics and gravity

*TORUS* uses a flux conserving, finite difference hydrodynamics algorithm. It is total variation diminishing (TVD), includes a Rhie–Chow interpolation scheme to prevent odd–even decoupling (Rhie & Chow 1983) and, in this paper, we use the van Leer flux limiter (van Leer 1979). The disc’s self-gravity is negligible and so we simply assume a point source potential determined by the star. Testing of the hydrodynamics algorithm in *TORUS* is given in Haworth & Harries (2012).

#### 3.2 Ionization parameter heating

We use an extension of the scheme implemented by Owen et al. (2012), where the temperature in any cell optically thin to the X-rays is prescribed as a function of ionization parameter

$$\xi = \frac{L_X}{nr^2}, \quad (3)$$

where  $L_X$ ,  $n$  and  $r$  are the X-ray luminosity, local number density and distance from the star at which the ionization parameter is being evaluated. The temperature function  $f(\xi)$  was determined by comparison with the Monte Carlo photoionization code *MOCASSIN* (Ercolano et al. 2003, 2008) and is given by

$$T_{\text{hot}} = \frac{10^{a_0 \log_{10}(\xi) + b_0 \log_{10}(\xi)^{-2}}}{1 + c_0 \log_{10}(\xi)^{-1} + d_0 \log_{10}(\xi)^{-2} + e_0} \quad (4)$$

$$T_{\text{cold}} = \max(10^{f_0 \log_{10}(\xi) + g_0}, T_{\text{dust}}) \quad (5)$$

$$f(\xi) = \min(T_{\text{hot}}, T_{\text{cold}}), \quad (6)$$

where the numerical constants (subscript 0) are included in Table 1. The resulting temperature–ionization parameter relation is shown in Fig. 1. We impose a minimum temperature of 10 K assuming that the ambient radiation field sets this floor value. This ionization parameter heating is applied to all cells that are optically thin, defined as those for which the column number density to the star is less than  $10^{22}$  particles  $\text{cm}^{-2}$  (Owen et al. 2010). In optically thin cells we set the temperature equal to the maximum of the temperature prescribed by  $f(\xi)$  and the local dust temperature. In cells optically thick to the X-rays the local dust temperature is applied (see Section 3.4).

**Table 1.** The constants used in the temperature-ionization parameter heating function (equations 4–6).

Constant	Value
$a_0$	$8.936\,252\,795\,924\,8299 \times 10^{-3}$
$b_0$	$-4.039\,242\,490\,536\,7275$
$c_0$	$12.870\,891\,083\,912\,458$
$d_0$	$44.233\,310\,301\,789\,743$
$e_0$	$4.346\,949\,695\,139\,6964$
$f_0$	$3.15$
$g_0$	$23.9$

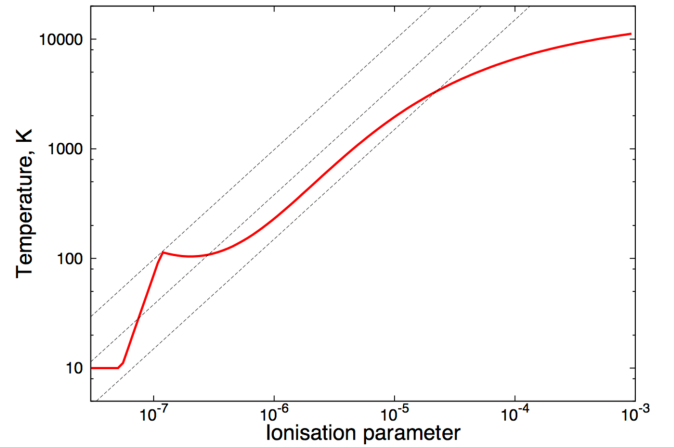


**Figure 1.** The temperature-ionization parameter prescription used for the calculations in this paper. It is constructed using equations 4–6 and the constants in Table 1. The diagonal lines represent lines of constant pressure.

##### 3.2.1 Limitations of our ionization parameter heating

The  $T(\xi)$  function used here is extended from the version used by Owen et al. (2012) down to lower values of  $\xi$ , using optically thin boxes in *MOCASSIN* calculations, where the role of attenuation is considered unimportant, until an imposed lower bound on the temperature of 10 K. This is the version used by Owen et al. (2013). Although we sample the whole viable range of  $\xi$ , once X-ray heating becomes relatively weak (i.e. for low  $\xi$ ) the effects of FUV heating and molecular cooling may also become important. Unfortunately FUV heating is not necessarily some simple function of the local properties, therefore in this work we only explore the effect of X-ray driven thermal sweeping described using the  $T(\xi)$  profile in Fig. 1. In this paper we will show that the detailed form in the low temperature regime (and in particular the existence of an implied pressure maximum) plays a much more important role in determining the onset of thermal sweeping than has been believed hitherto.<sup>1</sup>

In addition to missing lower temperature physics, this prescription assumes ionization equilibrium which may not always apply during fast-acting thermal sweeping.

<sup>1</sup> This finding is leading us to re-examine the detailed thermal structure of X-ray irradiated gas in the low X-ray flux, high density regime, which will be presented in future work. Here we study thermal sweeping using the previously adopted temperature-ionization parameter form of Owen et al. (2013). Thus, we strongly caution readers to be careful when considering the use of such a profile at low  $\xi$ .

### 3.3 Further implementation

We use a 2D cylindrical grid for all models in this paper. Since we assume reflective symmetry about the disc mid-plane we only model half of the disc (though we have checked this with simulations that do not assume reflective symmetry, finding any differences are negligible). In this implementation of TORUS we use a fixed, uniformly spaced, grid to ensure robust results (artificially induced instabilities can possibly arise on non-uniform or adaptive meshes, Fryxell et al. 2000). Our simulations are MPI parallelized and use domain decomposition. The RHDs uses operator splitting, i.e. we perform hydrodynamic and ionization parameter heating steps sequentially. We used a variety of total grid sizes and cell numbers, so the resolution varies. However, we always ensured that the disc scale-height at the radius of peak surface density is resolved by at least five cells. We checked for convergence in a test calculation using  $128^2$ ,  $256^2$  and  $512^2$  cells, finding good agreement, with marginally easier rapid clearing in the lower resolution simulations. For reference, the cell sizes are given in Table 3. We use a von Neumann–Richtmyer artificial viscosity scheme.

The models are initially allowed to evolve using hydrodynamics only, with the temperature set by the dust temperature only, until the disc settles into a steady state (typically up to five rotation periods at the inner disc rim).

### 3.4 Disc construction

We construct the disc by defining the peak mid-plane density  $\rho_{\max}$  at some radial distance  $R_{\max}$  (which can be translated into a surface density given the disc scaleheight). The mid-plane density  $\rho_{\text{mid}}$  is initially described by

$$\rho_{\text{mid}} = \rho_{\max} (R/R_{\max})^{-9/4}. \quad (7)$$

The dust temperature distribution is either taken from the models of D’Alessio, Calvet & Hartmann (2001), or is vertically isothermal and described by

$$T_d = \max \left( T_{1\text{au}} \left( \frac{R}{\text{au}} \right)^{-1/2}, 10 \right). \quad (8)$$

Equation (8) also reasonably describes the mid-plane temperature structure in the D’Alessio et al. (2001) models. We use two models in this paper, one with  $T_{1\text{au}} = 50$  K and one with  $T_{1\text{au}} = 100$  K. The vertical structure is initially constructed by imposing a profile corresponding to hydrostatic equilibrium for the case that the disc is vertically isothermal, i.e.

$$\rho(r, z) = \rho_{\text{mid}} \exp(-z^2/(2H^2)), \quad (9)$$

where  $H$  is the disc scaleheight  $c_s/\Omega$ . For the vertically isothermal models, this gives a surface density profile of the form

$$\Sigma(r) \propto R^{-1}. \quad (10)$$

The radial surface density profile for the models using the D’Alessio et al. (2001) temperature grid is similar, approximately of the form  $\Sigma(R) \propto R^{-0.93}$ .

The models in this paper are 2D cylindrically symmetric. We initially impose a Keplerian velocity profile for the azimuthal velocity, while the velocity in other directions is initially zero. The radial transition from disc to inner hole is initially not continuous; however, we begin the simulation run with hydrodynamics only (i.e. no radiation field) to allow the disc inner edge to relax. We set the  $\alpha$ -viscosity coefficient to a low value ( $10^{-6}$ ) as we do not expect secular evolution of the disc due to redistribution of angular

**Table 2.** Parameters used in our initial thermal sweeping test calculation, which is similar to that presented in Owen et al. (2012).

Parameter	Value	Description
$R_{\max}$	5 au	Inner hole radius
$\rho_{\max}$	$1 \times 10^{-14} \text{ g cm}^{-3}$	Peak mid-plane density
$T_{1\text{au}}$	50 K	1 au mid-plane dust temperature
$T_D(z > 0)$	D’Alessio	Vertical dust temperature profile
$M_*$	$0.1 M_{\odot}$	Star mass
$L_X$	$2 \times 10^{30} \text{ erg s}^{-1}$	X-ray luminosity
$\Sigma_{\max}$	$0.258 \text{ g cm}^{-2}$	Peak surface density

momentum on the time-scale on which the steady state wind solution is established. As with the simulations of Owen et al. (2012) we assume a constant mean particle mass of 1.37 over the whole simulation grid.

Once the disc is irradiated by X-rays, the properties of X-ray heated gas in the disc mid-plane and its interface with the dust heated disc can also be estimated semi-analytically using an approach which we discuss in the appendix.

## 4 CODE TESTING

TORUS is an extensively tested code (see e.g. Pinte et al. 2009; Haworth & Harries 2012; Bisbas et al. 2015; Harries 2015); however, for the applications in this paper, some new features have been added such as the ionization parameter heating function. We ran test calculations of stable discs to compare with expectations from Owen et al. (2012). We found mass-loss rates to within 40 per cent of the relation B4 from their work

$$\dot{M} = 4.8 \times 10^{-9} \left( \frac{M_*}{M_{\odot}} \right)^{-0.148} \left( \frac{L_X}{10^{30} \text{ erg s}^{-1}} \right)^{1.14} M_{\odot} \text{ yr}^{-1} \quad (11)$$

which was fitted to their simulations results. A deviation of 40 per cent is in line with the range of differences between the models and fit from Owen et al. (2012).

We also checked that the specific angular momentum and Bernoulli constant

$$\frac{v^2}{2} + \Psi + \int \frac{dp}{\rho} \quad (12)$$

were invariant along streamlines for a disc in a steady state, finding that these vary by less than 0.035 and 5 per cent along 80 au of any given streamline, respectively. The small variation in the Bernoulli constant arises both from the necessity of fitting a barotropic equation of state along the streamline in order to evaluate the  $\int dp/\rho$  term (resulting in interpolation error) and from small departures from a steady flow; these deviations are similar in magnitude to those found by Owen et al (2010).

As a further test, we also first consider a thermal sweeping scenario very similar to that in the original calculation presented in Owen et al. (2012). The parameters of this model (which has the same D’Alessio dust temperature structure and has a very similar peak mid-plane density and inner hole radius to the original model) are given in Table 2. Snapshots of the density evolution of this first model are given in Fig. 2. The morphological evolution is the same as that observed in the original thermal sweeping models. A billowy plume of material at the disc inner edge appears just prior to rapid disc clearing. Once the instability is fully initiated, over 20 au of the disc clears in about 700 years. We illustrate the accelerated clearing through Fig. 3: for a surface density profile given by



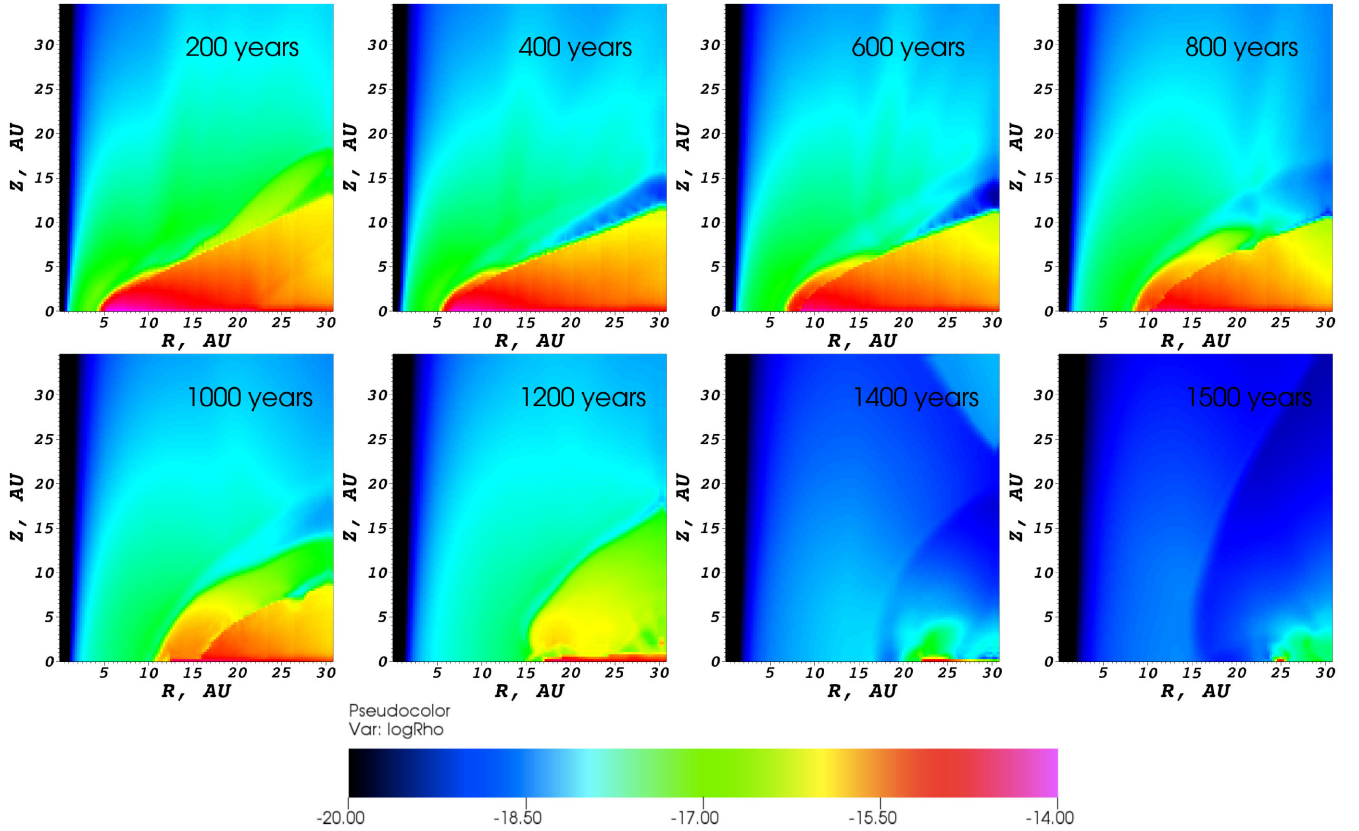


**Figure 2.** The evolution of the density distribution of a disc in the column limited regime. The disc is stable until a plume of material moving vertically at the disc inner edge allows the X-rays to propagate further into the disc.

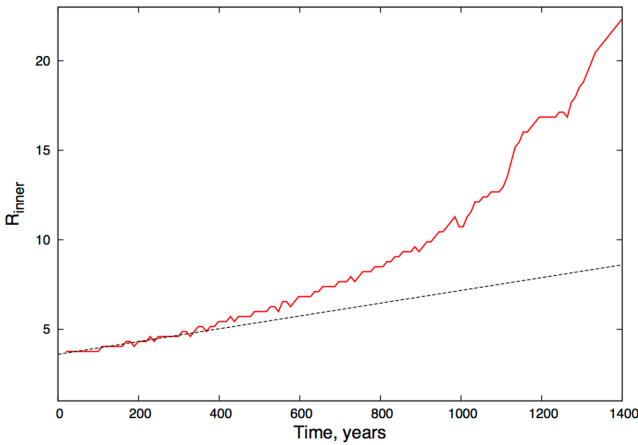


**Figure 3.** The evolution of the disc inner radius for our initial thermal sweeping test calculation, which has similar parameters to that presented in Owen et al. (2012). Note that once instability initiates, the disc inner radius increases non-linearly with time. The black line shows a linear evolution of the disc inner edge.

equation 10, constant mass-loss (as in the case of normal X-ray photoevaporation) results in a *linear* increase of inner hole radius with time as seen at times less than 300 years. Subsequently, the non-linear increase of disc radius with time indicates the transition to runaway clearing.

In summary, TORUS reproduces the behaviour expected from previously published simulations. It conserves physical constants accu-

rately and for stable and unstable discs is consistent with the results presented by Owen et al. (2012).

## 5 RESULTS

### 5.1 The suite of simulations

We ran a suite of 2D RHD simulations of disc photoevaporation using the procedure discussed in Section 3. This includes simulations in the column limited and density limited regimes. Since there are a large number of possible free parameters (i.e. all of those associated with the stellar and disc properties) and it is the evolution of the disc properties that should tip a given disc into the thermal sweeping regime, we predominantly focus on modifying the disc parameters rather than the stellar. We explore two different stellar masses ( $0.1$  &  $0.7 M_{\odot}$ ) and a range of disc inner hole radii and masses. All models consider an X-ray luminosity of  $2 \times 10^{30} \text{ erg s}^{-1}$ . A summary of the simulation parameters are given in Table 3. We run all models until it is clear whether normal clearing or radiative instability (i.e. non-linear inner hole growth) is occurring, with a maximum simulation time of about 6000 years.

### 5.2 Testing the Owen et al. (2013) criterion for the onset of thermal sweeping

In Fig. 4, we show the ratio of the peak disc surface density in our models to the surface density at which thermal sweeping is predicted to initiate according to the Owen et al. (2013) approach (equation 2 in this paper). The points are colour coded blue and red

**Table 3.** Summary of the parameters of the simulations in this paper.  $R_{\max}$  is the location of the peak mid-plane density, either in the long-term for a stable disc, or for an unstable disc that just prior to rapid clearing.  $\Sigma_{\max}$  is the surface density at  $R_{\max}$ .  $T_{1\text{au}}$  is the dust temperature at 1 au.  $\rho_{\max}$  is the mid-plane density at  $R_{\max}$ . All models have  $L_X = 2 \times 10^{30} \text{ erg s}^{-1}$ .

Model ID	Stellar mass $M_{\odot}$	$R_{\max}$ au	$\Sigma_{\max}$ $\text{g cm}^{-2}$	$T_{1\text{au}}$ K	$\rho_{\max}$ $\text{g cm}^{-3}$	Column limited?	Vertically isothermal?	Stable?	resolution au
A	0.7	28.1	7.2	100	$1.20 \times 10^{-13}$	No	Yes	Yes	0.4
B	0.7	28.5	0.72	100	$1.20 \times 10^{-14}$	No	Yes	Yes	0.4
C	0.7	29.1	0.34	100	$5.50 \times 10^{-15}$	No	Yes	Yes	0.4
D	0.7	29.1	$7 \times 10^{-2}$	100	$1.26 \times 10^{-15}$	No	Yes	Yes	0.4
E	0.7	35.5	0.136	100	$6.77 \times 10^{-16}$	No	No	Yes	0.4
F	0.7	35.5	$2.8 \times 10^{-2}$	100	$3.40 \times 10^{-16}$	No	No	No	0.4
G	0.7	20.8	0.20	100	$4.62 \times 10^{-16}$	No	No	No	0.4
H	0.7	26.0	$5.2 \times 10^{-2}$	100	$5.81 \times 10^{-16}$	No	No	No	0.4
I	0.1	11.0	5.8	50	$1.34 \times 10^{-14}$	No	No	Yes	0.4
J	0.1	7.9	1.32	50	$2.94 \times 10^{-14}$	Yes	Yes	Yes	0.2
K	0.1	7.7	0.174	50	$1.26 \times 10^{-14}$	Yes	Yes	No	0.1
L	0.1	7.0	0.52	50	$1.20 \times 10^{-14}$	Yes	No	No	0.1
M	0.1	8.6	0.166	50	$7.41 \times 10^{-15}$	Yes	Yes	No	0.2
N	0.1	7.6	0.28	50	$8.22 \times 10^{-15}$	Yes	Yes	No	0.2
O	0.1	7.0	$9 \times 10^{-2}$	50	$4.49 \times 10^{-15}$	Yes	No	No	0.1
P	0.1	25	0.2	50	$2.0 \times 10^{-15}$	No	Yes	No	0.4
Q	0.1	25	2	50	$2.0 \times 10^{-14}$	No	Yes	Yes	0.4

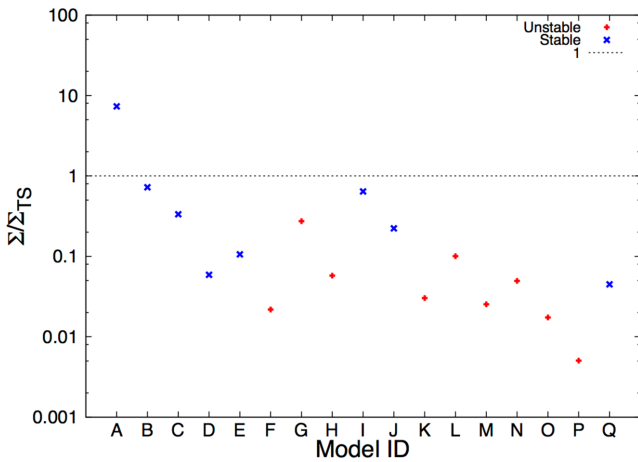


**Figure 4.** The ratio of the model peak surface density to the critical surface density for thermal sweeping according to the Owen et al. (2013) approach – equation 2 in this paper. Stable and unstable models should be separated by a ratio value of unity.

for stable and unstable models, respectively. An accurate criterion should separate the stable and unstable models about a ratio value of 1. The Owen et al. (2013) approach predicts that all models except model A should be unstable; however, this is certainly not the case in the simulations.

There are two possible reasons why this surface density threshold fails to distinguish stable and unstable models. The first is that the criterion on which this surface density is based (i.e.  $\Delta/H = 1$ ; see Section 1) is incorrect. The other is that the error might be introduced in going from this requirement to a corresponding column density; the latter step depends on the vertical structure of the disc and is therefore not unique for given mid-plane properties. We can distinguish these possibilities by examining the  $\Delta/H$  values corresponding to each model (Fig. 5). We do not measure  $\Delta/H$  directly from the simulations because there is no steady state for those simulations that turn out to be unstable. Instead we follow Owen et al (2013) in deriving analytic expressions for the predicted values of  $\Delta/H$  as a function of conditions at the cavity rim (see Appendix).

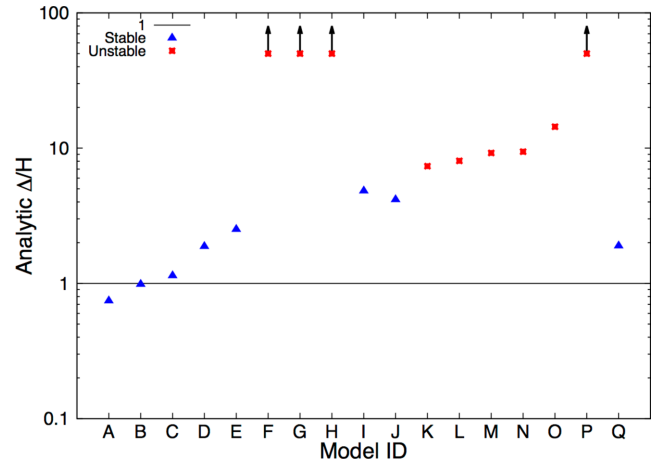


**Figure 5.** Analytic values of  $\Delta/H$  for the simulations in this paper. Blue and red points are stable and unstable, respectively. According to the existing theory,  $\Delta/H > 1$  should result in an unstable disc, however these results do not reflect this.

Fig. 5 again colour codes the simulation outcomes, with blue and red being stable and unstable, respectively. Note that we place an upper limit on  $\Delta/H$  in this plot, as the ratio can become very large. Analytically derived  $\Delta/H$  values give rise to predictions about the stability of the models consistent with the surface density estimate, in that almost all models are expected to become unstable. We thus demonstrate that the reason that the density threshold proposed by Owen et al. (2013) does not work is because  $\Delta/H = 1$  is apparently not the fundamental criterion for instability.

Since Fig. 5 suggests that, out of the models run, stable and unstable models are separated at about  $\Delta/H \sim 5$ , it is perhaps tempting to modify the criterion by just proposing a higher  $\Delta/H$  threshold; we do not do this because we shall see that the value of  $\Delta/H$  can be very insensitive to disc surface density. We illustrate this in Fig. 6, where we take a set of models with stellar and disc parameters identical to model Q but simply change the surface density normalization. The blue-black curve shows that it is possible to vary the disc column density normalization by two orders of

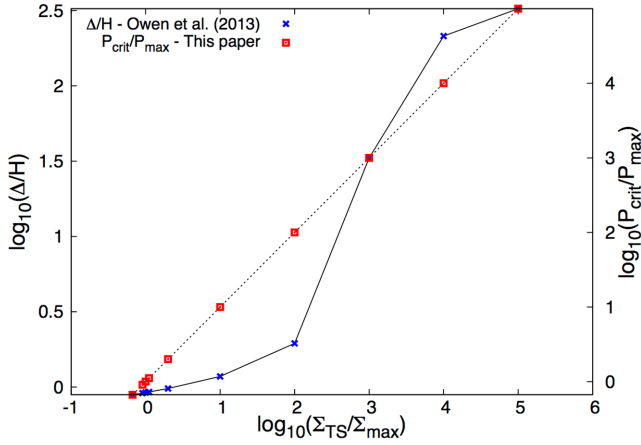


**Figure 6.** The variation in  $\Delta/H$  (left axis, blue-black line) or the ratio of critical to peak mid-plane pressure (right axis, red-black line) as a function of peak surface density for a disc with a 25 au inner hole about a  $0.1 M_{\odot}$  star with  $L_X = 2 \times 10^{30} \text{ erg s}^{-1}$ . Close to  $\Delta/H = 1$ , the ratio is not very sensitive to changes in the disc peak surface density. Conversely, the pressure ratio scales linearly over all surface densities.

magnitude while only affecting the value of  $\Delta/H$  by less than a factor 2. Thus a criterion based on the value of  $\Delta/H$  is likely to be highly inaccurate in predicting the threshold column density for the onset of thermal sweeping.

### 5.3 A new criterion for thermal sweeping

We have developed a new criterion for thermal sweeping which is consistent with all the simulations and which is based on the maximum pressure that can be attained by X-ray heated gas. Fig. 1 depicts a set of isobars in the plane of ionization parameter against temperature, with pressure rising towards the upper left of the plot. Evidently there is a maximum possible pressure  $P_{X\text{max}}$  (at fixed X-ray flux) which is associated with the feature in the ionization parameter versus temperature relation at  $\xi \sim 1 \times 10^{-7}$  and a temperature of  $\sim 100 \text{ K}$ . The existence of this maximum pressure places an absolute upper limit on the extent to which the X-ray heated region can penetrate into the disc. If the maximum pressure of X-ray heated gas is less than the maximum disc mid-plane pressure  $P_{D\text{max}}$  at the inner rim then there is no means by which the disc can be engulfed by a front of runaway X-ray heating. We might therefore expect that  $P_{X\text{max}} < P_{D\text{max}}$  is a *sufficient* condition for stability.

We can also assess whether  $P_{X\text{max}} < P_{D\text{max}}$  should be a *necessary* condition for stability, i.e. whether there are also stable solutions where  $P_{X\text{max}} > P_{D\text{max}}$  but where the interface between X-ray heated and disc gas occurs at a pressure  $P_i < P_{D\text{max}}$ . We, however, argue that such an interface would be unstable since perturbations would drive the solution up the steep branch of the ionization parameter temperature plot at  $\xi < 10^{-7}$ . Pressure is a negative function of density along this branch and therefore underdense regions can evolve up the branch towards the pressure maximum. The radial extent of such excursions is however limited if  $P_{X\text{max}} < P_{D\text{max}}$ . We, therefore, propose that this is both a necessary and sufficient condition for stability.

We test this hypothesis in Fig. 7 where again stable and unstable models are colour coded and we plot the ratio of the maximum pressure in the dust heated disc to  $P_{X\text{max}}$ :

$$P_{X\text{max}} = P_{\text{TS}} = \frac{L_X}{\xi_{\text{crit}} R_{\text{max}}^2} k_B T_{\text{crit}}, \quad (13)$$

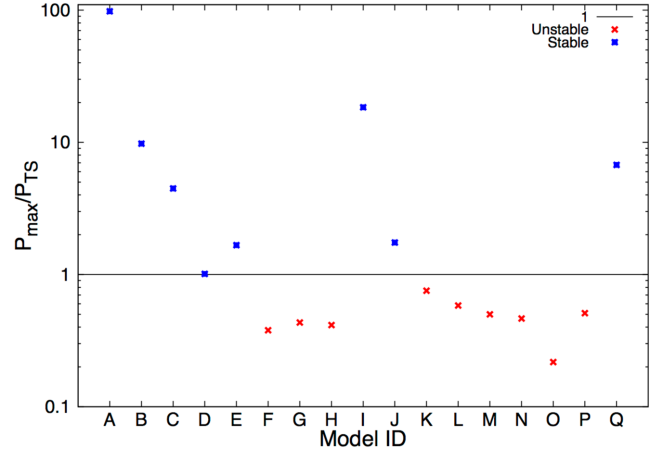


**Figure 7.** The ratio of the disc maximum mid-plane pressure to the critical pressure for rapid radiative disc dispersal (equation 13). There is a clear transition from instability to stability once the ratio exceeds unity.

where  $\xi_{\text{crit}}$  and  $T_{\text{crit}}$  are the temperature and ionization parameter corresponding to the maximum pressure attainable by X-ray heated gas. From the temperature–ionization parameter relation, we find that  $\xi_{\text{crit}} = 1.2 \times 10^{-7}$  and  $T_{\text{crit}} = 113 \text{ K}$ . We see that the ratio  $P_{X\text{max}}/P_{D\text{max}}$  is indeed an excellent discriminant between stable and unstable models. Furthermore, in Fig. 6 the black-red line shows the variation of the pressure ratio for a disc with a 25 au hole (i.e. similar to model Q) at different surface density normalizations. Note that we have already argued that for such a disc  $\Delta/H$  is not always sensitive to changes in the surface density, making it a poor criterion. Conversely, our new criterion scales linearly with the disc surface density.

It is important to note that under this new criterion thermal sweeping depends on the form of the low  $\xi$  end of the  $T(\xi)$  function. If FUV heating dominates in these regions, then this region of  $T(\xi)$  may not be accessible to the disc and the physics controlling thermal sweeping is likely to be qualitatively different. It will be important to assess the role of FUV heating and molecular cooling in future work.

For this critical pressure criterion, the corresponding critical peak mid-plane volume density for thermal sweeping is

$$n_{\text{TS}} = 4.2 \times 10^{10} \text{ cm}^{-3} \left( \frac{R_{\text{max}}}{\text{au}} \right)^{-3/2} \left( \frac{T_{1\text{au}}}{100} \right)^{-1} \left( \frac{L_X}{10^{30}} \right). \quad (14)$$

Although, we go on to discuss critical surface densities, it is important to emphasize that thermal sweeping is actually determined by a criterion on the volume density, not the surface density. One could therefore conceive of two discs with identical surface densities, but different thermal structures such that the mid-plane density differs sufficiently that one disc is stable and the other unstable. Nevertheless, in practice a surface density criterion for thermal sweeping is more accessible and more useful than a volume density estimate. The D’Alessio models (in which the temperature rises above the mid-plane) have a higher surface density at fixed mid-plane density than a vertically isothermal model and thus assuming a vertically isothermal disc to calculate the critical surface density for thermal sweeping should provide a reasonable lower limit. Hence, we approximate

$$\Sigma_{\text{TS}} = 2\rho_{\text{TS}} \frac{c_s}{\Omega} \quad (15)$$

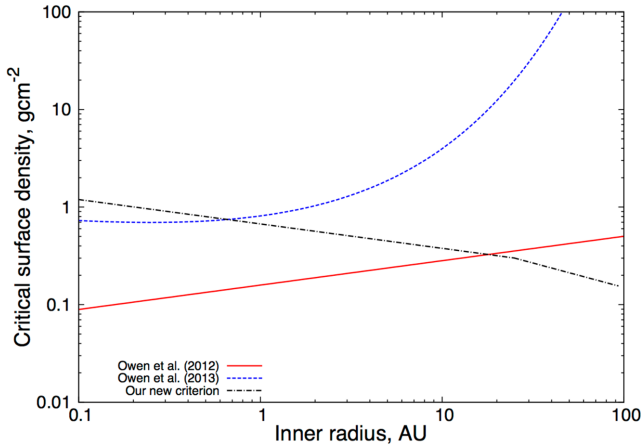


**Figure 8.** A comparison of the critical surface density for thermal sweeping from Owen et al. (2012, 2013) and the new relation derived here. Note that these relations assume a vertically isothermal disc and will likely be a lower limit for warmer discs with lower mid-plane densities. This plot assumes  $T_X = 400$  K,  $T_{1\text{au}} = 50$  K and  $M_* = 0.1 M_\odot$ .

which, using equation 14, assuming  $\mu = 1.37$  and inserting other constants, results in

$$\Sigma_{\text{TS}} = 0.075 \text{ g cm}^{-2} \left( \frac{L_X}{10^{30}} \right) \left( \frac{M_*}{M_\odot} \right)^{-1/2} \times \left( \frac{T_{1\text{au}}}{100} \right)^{-1/2} \left( \frac{R_{\text{max}}}{\text{au}} \right)^{-1/4}. \quad (16)$$

Interestingly, this criterion is very similar to the expression derived using the Owen et al. (2013) approach (equation 2) but without the exponential term. This difference can be readily understood in that we now just require for stability that the pressure in the dust heated disc exceeds the maximum pressure of X-ray heated gas; Owen et al. (2013) proposed a more stringent requirement for stability by additionally placing constraints on the scalelength of X-ray heated gas, a condition that required that the interface was a sufficiently large number of pressure scalelength from the disc pressure maximum. Our criterion is more readily satisfied and we therefore find a lower surface density threshold for thermal sweeping than Owen et al 2013.

Although the disc temperature in our simulations scales as  $R^{-1/2}$ , we set the disc temperature to a floor value of 10 K at radii beyond

$$R_{\text{floor}} = 1 \text{ au} \left( \frac{T_{1\text{au}}}{10} \right)^2 \quad (17)$$

and so beyond  $R_{\text{floor}}$  the critical surface density for thermal sweeping is

$$\Sigma_{\text{TS}} = 0.24 \text{ g cm}^{-2} \left( \frac{L_X}{10^{30}} \right) \left( \frac{M_*}{M_\odot} \right)^{-1/2} \left( \frac{R_{\text{max}}}{\text{au}} \right)^{-1/2}. \quad (18)$$

We reiterate that these surface density estimates assume a vertically isothermal disc.

We compare this new composite relation (equations 16, 18) alongside the Owen et al. (2012) and Owen et al. (2013) expressions in Fig. 8. In constructing Fig. 8 we assume that  $T_X = 400$  K (for the Owen et al. 2012 criterion),  $T_{1\text{au}} = 50$  K and  $M_* = 0.1 M_\odot$  (and that the disc is vertically isothermal). We see that, unlike the criteria previously proposed, our new critical surface density threshold declines (albeit mildly) with radius and thus sweeping at large radius is harder than for the previous prescriptions. On the other hand, it is

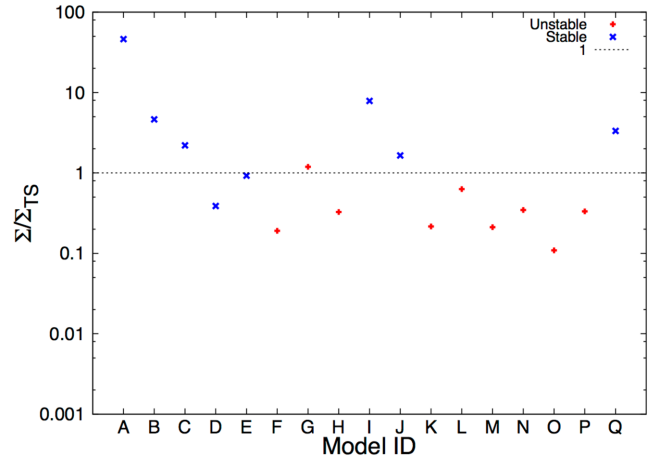


**Figure 9.** The ratio of the model peak surface density to the critical surface density for thermal sweeping according to our new criterion – equation 22 in this paper. Stable and unstable models should be separated by a ratio value of unity. The new criterion is much more accurate than the old (see Fig. 4). The small discrepancies are consistent with the way that changes in the assumed vertical structure affect the mapping from mid-plane to vertically integrated quantities.

important to note that the radial decrease of the disc surface density in our simulations (and also in observed discs – Andrews et al. 2009) is *steeper* ( $\Sigma \propto R^{-1}$ ) than the radial decrease in the critical surface density ( $\Sigma \propto R^{-1/4}$  or  $\Sigma \propto R^{-1/2}$ ). This means that a disc that becomes unstable to rapid radiative clearing at small radii should then clear out the whole disc. It also means that, for canonical disc surface density profiles, thermal sweeping will always eventually set in at some large radius in the disc.

We reiterate that the actual criterion is on the peak mid-plane pressure and hence the volume density, not the surface density. We should therefore not expect the new surface density criterion to be completely accurate. In Fig. 9, we show the ratio of the model peak surface density to the critical surface density for thermal sweeping given by our new criterion. Compared with the old criterion (see Fig. 4) there is much better agreement: the new solution is accurate to within a factor of 2, even though the surface density is not the fundamental parameter.

## 6 DISCUSSION

### 6.1 The clearing radius for discs with holes opened by photoevaporation

Combining the theory of normal disc photoevaporation detailed by Owen et al. (2010, 2011, 2012) with the theory of viscous disc accretion presented by Hartmann et al. (1998) we can constrain the maximum possible inner hole radius for viscous discs with inner holes opened by photoevaporation (cf. Alexander et al. 2006b). For normal photoevaporation, to zeroth order the photoevaporative mass-loss rate

$$\dot{M}_w = 8 \times 10^{-9} \left( \frac{L_X}{10^{30}} \right) M_\odot \text{ yr}^{-1} \quad (19)$$

is approximately equal to the accretion rate at gap opening (Alexander et al. 2006b; Owen et al. 2011) and we can ignore the effects of photoevaporation on the previous evolution of the disc. Using the self-similar disc evolution model for  $\nu \propto R$  given by



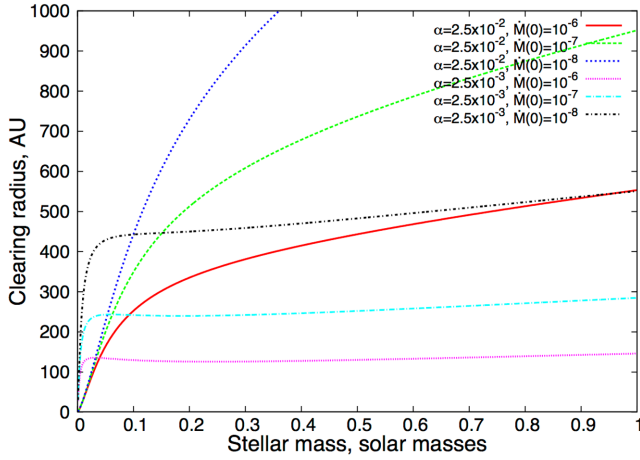


**Figure 10.** The radius beyond which rapid disc clearing would take place as a function of the mass of the central source, for discs undergoing normal internal photoevaporation and viscous accretion.

Lynden-Bell & Pringle (1974); Hartmann et al. (1998), at the time of gap opening the surface density profile is

$$\Sigma_{\text{GO}} = \frac{M_d(0)}{2\pi R R_1} T_{\text{GO}}^{-3/2} \exp\left(-\frac{R}{R_1 T_{\text{GO}}}\right). \quad (20)$$

Here,  $T$  denotes normalized time ( $T = 1 + t/t_s$ ) where  $t_s$  is the viscous time at the initial characteristic radius of the disc ( $R_1$ ) and the subscript GO denotes the normalized time at gap opening. By equating equation 20 with the evolution of the accretion rate in the viscous similarity solution we obtain:

$$T_{\text{GO}} = \left(\frac{M_d(0)}{2t_s \dot{M}_w}\right)^{2/3}. \quad (21)$$

Once the gap is opened, then the disc profile remains roughly constant, and described by equation 20 during the time that photoevaporation erodes the inner hole. Thus equating equation 20 to the thermal sweeping criterion (equation 16) we can solve for the radius at which thermal sweeping will initiate for a viscous accretion disc undergoing photoevaporation. In practice it turns out that thermal sweeping occurs in the region of the disc where the radial exponential fall-off (equation 20) is important. This means that the radius for thermal sweeping cannot be written in closed form and requires numerical solution. In Fig. 10 we plot the full numerically evaluated solution. We assume that the initial disc mass  $M_d(0)$  is 10 per cent of the stellar mass. We use the fit to the dependence of mean X-ray luminosity on stellar mass of Preibisch et al. (2005), i.e.

$$\log_{10}(L_X) = 30.37 + 1.44 * \log_{10}(M_*/M_{\odot}). \quad (22)$$

We also derive  $T_{1\text{au}}$  as a function of stellar mass by linear interpolation of the values used for the simulations in this paper (i.e. 50 and 100 K for 0.1 and 0.7  $M_{\odot}$  stars, respectively). We assign values of  $R_1$  in equation 24 by assuming a value of  $\alpha$  and an initial mass accretion rate, since

$$\frac{M_d(0)}{2t_s} = \dot{M}(0) \quad (23)$$

from Hartmann et al. (1998) gives

$$\left(\frac{R_1}{\text{au}}\right) = 63.6 \left(\frac{M_d(0)}{0.1 M_{\odot}}\right) \left(\frac{\alpha}{10^{-2}}\right) \left(\frac{T_{1\text{au}}}{100}\right) \times \left(\frac{M_*}{M_{\odot}}\right)^{-1/2} \left(\frac{\dot{M}(0)}{10^{-7} M_{\odot} \text{yr}^{-1}}\right)^{-1}. \quad (24)$$

Fig. 10 shows the resulting numerical solution for a range of  $\alpha$  and  $\dot{M}(0)$  values. Lower viscosities and higher initial mass accretion rates are more conducive to thermal sweeping, though in general it only ever initiates at very large radii and should have little bearing on the overall evolution of such normal discs.

Note that we have ignored viscous spreading and the removal of mass due to photoevaporation prior to gap opening and have therefore slightly overestimated the disc surface densities at gap opening. Nevertheless, the modest depletion of gas by photoevaporation prior to gap opening (Owen et al 2011) will not dramatically reduce the very large clearing radii reported here.

Although normal viscous accretion and internal photoevaporation is unlikely to lead to thermal sweeping, it could still arise if some other process such as planet formation can lower the peak surface density below the critical value.

## 6.2 Population synthesis models

Since our new calculations suggested that Owen et al (2013) overestimated the surface density at which thermal sweeping sets in, it is important to quantify the effect a much less efficient thermal sweeping process would have on a population of evolving discs. Owen et al. (2012, 2013) suggested that thermal sweeping would destroy the outer disc almost immediately after photoevaporation had opened a gap in the inner disc and it had drained on to the central star. Such rapid destruction was necessary to avoid producing a large number of non-accreting transition discs with large holes, and was consistent with the transition disc statistics.

The large radii that we estimate for the onset of thermal sweeping in Fig. 10 lead us to now expect that thermal sweeping will do little to help avoid the overprediction of relic gas discs at large radii. We confirm this by applying our new thermal sweeping criterion to the synthetic disc population of Owen et al. (2011). This population evolved under the action of viscosity and X-ray photoevaporation starting from a single disc model (a Lynden-Bell & Pringle 1974, zero time similarity solution). It was designed to match the general observational properties of disc evolution (disc fraction and accretion rate evolution as a function of time). Variety in disc evolution came from the spread in X-ray luminosities alone, which in turn created a spread in photoevaporation rates. We post-process this simulation set, which did not originally include thermal sweeping and the disc was entirely destroyed by standard photoevaporation. After the gap has opened and the inner disc has drained, we assume thermal sweeping takes place once the peak surface density in the remaining outer disc drops below the threshold given in equation (16). We then record the inner hole radius where this occurred, the remaining disc mass and the lifetime over which the disc would have appeared as an accreting and non-accreting transition disc.

Fig. 11 shows histograms of the ratio of the non-accreting transition disc lifetime to the accreting transition disc lifetime for individual discs (left-hand panel) and the inner hole radius at which thermal sweeping initiates (right-hand panel). The inner hole radii at which thermal sweeping begins is around  $\sim 300$  au, consistent with the general picture discussed above. These clearing radii are significantly bigger than the  $\leq 40$  au found by Owen et al. (2013). As shown in the left-hand panel of Fig. 11 this results in the majority of discs spending a large fraction of time as a non-accreting transition disc with a large hole. We find thermal sweeping only initiates once the hole radius becomes comparable with the outer radius of the disc and the surface density begins to drop exponentially rather than with an  $R^{-1}$  powerlaw. The remaining disc mass at this point is

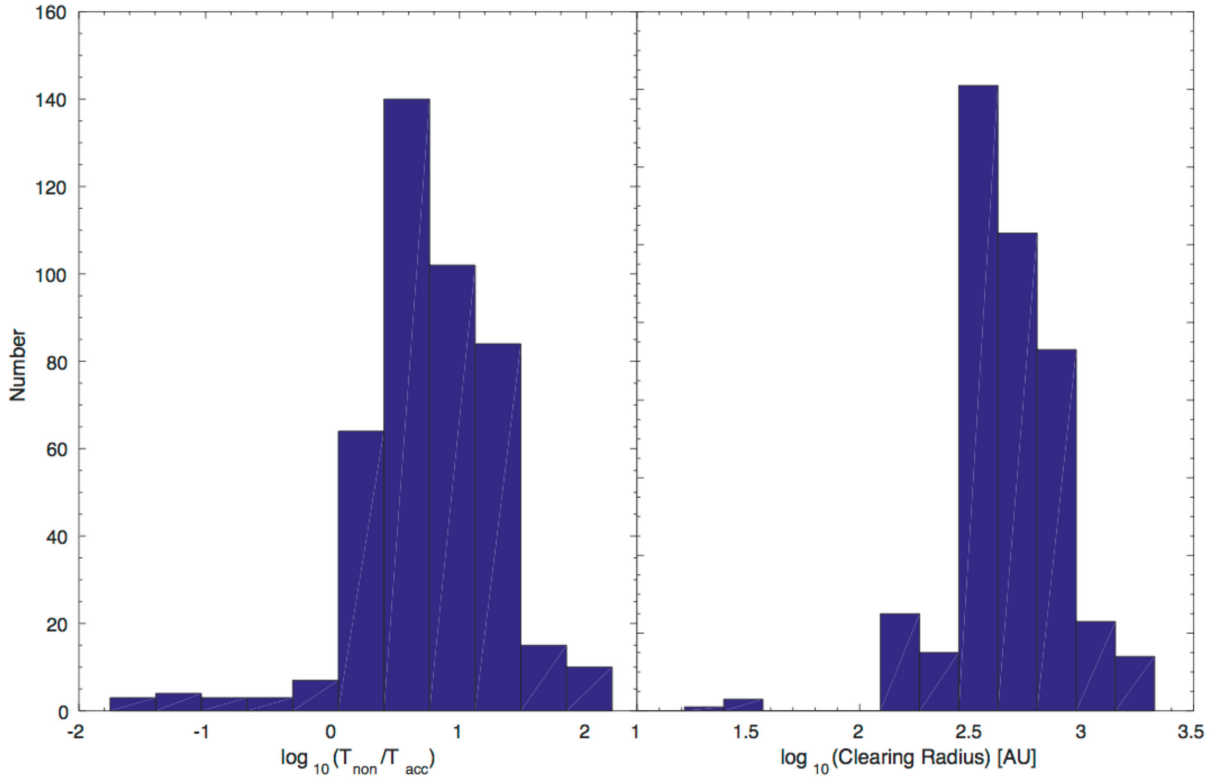


**Figure 11.** Histograms showing the ratio of the non-accreting to accreting transition disc lifetimes (left-hand panel) and inner hole radii at which thermal sweeping initiates (right-hand panel). For a population of discs evolving under the combined action of viscosity, X-ray photoevaporation and the new thermal sweeping criterion given in equation (16).

small  $\sim 10^{-5} - 10^{-4} M_{\odot}$ . In fact we find that with this revised thermal sweeping criterion, thermal sweeping has little impact on the total evolution of the disc and without thermal sweeping the remaining disc would be quickly removed by ordinary photoevaporation. The small number of discs with a small rapid clearing radius have the highest photoevaporation rates. For large hole radii ( $> 20$  au) the number of non-accreting (or those with upper limits) to accreting transition discs is observed to be small  $\sim 20$  per cent (Williams & Cieza 2011). Therefore, it appears X-ray driven thermal sweeping is unable to effectively destroy the final remnant disc as previously hypothesised. It is possible that other components of the radiation field not considered here, such as the FUV, play an important role in the final evolution of protoplanetary discs (e.g. Gorti et al. 2015).

## 7 SUMMARY AND CONCLUSIONS

We have used RHD simulations to investigate the final, rapid, radiative clearing of gas from protoplanetary discs. We draw the following main conclusions from this work.

(1) Rapid radiative clearing does not fundamentally occur when the ratio of vertical and radial pressure scalelengths  $\Delta/H = 1$ , as proposed by Owen et al. (2012, 2013). Rather it hinges upon the requirement that the maximum pressure attainable by X-ray heated gas must be less than the pressure in the dust heated disc at its maximum (near the disc inner edge).

(2) We present an equation for the critical volume density (equation 14) for rapid radiative clearing, as well as a lower limit critical surface density expression (equation 16), based on an assumed vertically isothermal temperature profile in the disc. Our new critical

surface density estimate is both quantitatively and qualitatively different to the previous estimates of Owen et al. (2012, 2013) and, generally, will result in thermal sweeping happening less readily than previously expected (see Fig. 8).

(3) We use the previously established theory of disc photoevaporation to calculate the maximum possible inner hole radius as a function of the stellar mass, for viscous discs with gaps opened by photoevaporation. We find that thermal sweeping only happens at radii where it can have a significant impact on disc evolution for low  $\alpha$  parameters and high initial accretion rates. Even in this regime, thermal sweeping only initiates beyond 100 au. It is still possible that some other mechanism could reduce the disc surface density sufficiently that thermal sweeping initiates at smaller radii.

(4) Since rapid radiative clearing happens less readily than previously believed, the time discs spend in the non-accreting phase will be longer than estimates such as those by Rosotti et al. (2015).

(5) X-ray driven thermal sweeping does not appear to be the solution to the lack of non-accreting transition discs with large holes. Thus, further work is required to explain the apparent speed up of outer disc dispersal following the shut-off of accretion on to the central star and clearing of the inner disc. In particular it is possible that FUV heating, which may dominate in components of the disc where X-ray heating is weak but is not included here, could play an important role in the final clearing of protoplanetary discs.

## ACKNOWLEDGEMENTS

We thank the referee, Barbara Ercolano, for her swift but insightful review of the paper, which also highlighted important avenues for future research. We also thank Giovanni Rosotti and Stefano

Facchini for useful discussions. TJH is funded by the STFC consolidated grant ST/K000985/1. Support for CJC and additional hardware costs are provided by the DISCSIM project, grant agreement 341137 funded by the European Research Council under ERC-2013-ADG. JEO acknowledges support by NASA through Hubble Fellowship grant HST-HF2-51346.001-A awarded by the Space Telescope Science Institute, which is operated by the Association of Universities for Research in Astronomy, Inc., for NASA, under contract NAS 5-26555. This work was undertaken on the COSMOS Shared Memory system at DAMTP, University of Cambridge operated on behalf of the STFC DiRAC HPC Facility. This equipment is funded by BIS National E-infrastructure capital grant ST/J005673/1 and STFC grants ST/H008586/1, ST/K00333X/1. DiRAC is part of the National E-Infrastructure.

## REFERENCES

- Alexander R. D., Clarke C. J., Pringle J. E., 2006a, *MNRAS*, 369, 216  
 Alexander R. D., Clarke C. J., Pringle J. E., 2006b, *MNRAS*, 369, 229  
 Andrews S. M., Wilner D. J., Hughes A. M., Qi C., Dullemond C. P., 2009, *ApJ*, 700, 1502  
 Andrews S. M., Wilner D. J., Espaillat C., Hughes A. M., Dullemond C. P., McClure M. K., Qi C., Brown J. M., 2011, *ApJ*, 732, 42  
 Bisbas T. G. et al., 2015, *MNRAS*, 453, 1324  
 Bruderer S., van der Marel N., van Dishoeck E. F., van Kempen T. A., 2014, *A&A*, 562, A26  
 Calvet N., D'Alessio P., Hartmann L., Wilner D., Walsh A., Sitko M., 2002, *ApJ*, 568, 1008  
 Cieza L. A. et al., 2013, *ApJ*, 762, 100  
 Clarke C. J., Gendrin A., Sotomayor M., 2001, *MNRAS*, 328, 485  
 D'Alessio P., Calvet N., Hartmann L., 2001, *ApJ*, 553, 321  
 Dullemond C. P., Dominik C., Natta A., 2001, *ApJ*, 560, 957  
 Ercolano B., Barlow M. J., Storey P. J., Liu X., 2003, *MNRAS*, 340, 1136  
 Ercolano B., Young P. R., Drake J. J., Raymond J. C., 2008, *ApJS*, 175, 534  
 Ercolano B., Clarke C. J., Drake J. J., 2009, *ApJ*, 699, 1639  
 Fryxell B. et al., 2000, *ApJS*, 131, 273  
 Gorti U., Hollenbach D., 2009, *ApJ*, 690, 1539  
 Gorti U., Hollenbach D., Dullemond C. P., 2015, *ApJ*, 804, 29  
 Haisch K. E., Jr, Lada E. A., Lada C. J., 2001, *ApJ*, 553, L153  
 Hardy A. et al., 2015, *A&A*, 583, A66  
 Harries T. J., 2000, *MNRAS*, 315, 722  
 Harries T. J., 2015, *MNRAS*, 448, 3156  
 Hartmann L., Calvet N., Gullbring E., D'Alessio P., 1998, *ApJ*, 495, 385  
 Haworth T. J., Harries T. J., 2012, *MNRAS*, 420, 562  
 Haworth T. J., Harries T. J., Acreman D. M., Bisbas T. G., 2015, *MNRAS*, 453, 2277  
 Hollenbach D., Johnstone D., Lizano S., Shu F., 1994, *ApJ*, 428, 654  
 Koepferl C. M., Ercolano B., Dale J., Teixeira P. S., Ratzka T., Spezzi L., 2013, *MNRAS*, 428, 3327  
 Lynden-Bell D., Pringle J. E., 1974, *MNRAS*, 168, 603  
 Owen J. E., Ercolano B., Clarke C. J., Alexander R. D., 2010, *MNRAS*, 401, 1415  
 Owen J. E., Ercolano B., Clarke C. J., 2011, *MNRAS*, 412, 13  
 Owen J. E., Clarke C. J., Ercolano B., 2012, *MNRAS*, 422, 1880  
 Owen J. E., Clarke C. J., 2012, *MNRAS*, 426, L96  
 Owen J. E., Hudoba de Badyn M., Clarke C. J., Robins L., 2013, *MNRAS*, 436, 1430  
 Pinte C., Harries T. J., Min M., Watson A. M., Dullemond C. P., Woitke P., Ménard F., Durán-Rojas M. C., 2009, *A&A*, 498, 967  
 Preibisch T. et al., 2005, *ApJS*, 160, 401  
 Rhie C. M., Chow W. L., 1983, *Am. Inst. Aeronaut. Astronaut. J.*, 21, 1525  
 Rice W. K. M., Armitage P. J., 2003, *ApJ*, 598, L55  
 Rosotti G. P., Ercolano B., Owen J. E., 2015, *MNRAS*, 454, 2173  
 van der Marel N., van Dishoeck E. F., Bruderer S., Pérez L., Isella A., 2015, *A&A*, 579, A106  
 van Leer B., 1979, *J. Comput. Phys.*, 32, 101  
 Williams J. P., Cieza L. A., 2011, *ARA&A*, 49, 67

## APPENDIX A: CALCULATING THE DISC MID-PLANE PROPERTIES SEMI-ANALYTICALLY

Here, we summarize a particularly useful semi-analytic tool for studying the radial variation of the disc mid-plane properties. At each radius  $R$  in the disc the cold, dust-temperature dominated, properties of the gas are number density

$$n_D = n_{\max} \left( \frac{R}{R_{\max}} \right)^{-9/4} \quad (\text{A1})$$

temperature

$$T_D = \max \left( T_{\text{lau}} \left( \frac{R}{\text{au}} \right)^{-0.5}, 10 \right) \quad (\text{A2})$$

and pressure

$$P_D = n_D k_B T_D. \quad (\text{A3})$$

Conversely the X-ray irradiated properties are the number density  $n_X$  (to be determined), the temperature

$$T_X = f(\xi) \quad (\text{A4})$$

(see equation 6) and pressure

$$P_X = n_X k_B T_X. \quad (\text{A5})$$

Combining equations 9 and 11 from Owen et al. (2013), the radial pressure scalelength is given by

$$\Delta = \frac{c_X^2}{\sqrt{2} c_D \Omega \sqrt{\log(P_D/P_X)}}, \quad (\text{A6})$$

where  $\Omega$  is the angular velocity at a given radius. Note that due to the pressure ratio, this semi-analytic approach does not function when the X-ray pressure is larger the dust pressure (which may be the case in very low density discs).

In order to solve for the conditions we have to iterate over possible reasonable values of  $n_X$  to calculate  $\xi$ ,  $T_X$  and  $\Delta$ . Interior to some radius  $R_{\text{crit}}$ ,  $n_X \Delta$  never drops below  $10^{22}$ , we are in the column limited case and so we set  $n_X = 10^{22}/\Delta$  by construction, allowing us to calculate the conditions as a function of radius (including  $\xi$ ,  $\Delta$ ,  $H$  and therefore  $\Delta/H$  assuming vertical isothermality).

Once  $n \Delta$  drops below  $10^{22}$  we have located the transition to being density limited. From here outwards, the ionization parameter is some minimum value  $\xi_{\min}$ , which is approximately  $3 \times 10^{-7}$ . We can then calculate the number density as

$$n_X = \frac{L_X}{\xi_{\min} R^2} \quad (\text{A7})$$

and hence can then calculate all parameters as a function of radius beyond the density limited transition radius.

This paper has been typeset from a  $\text{\LaTeX}$  file prepared by the author.